Contribuciones del Instituto Nacional de Investigaciones Nucleares al avance de la Ciencia y la Tecnología en México

Edición conmemorativa 2010

Chapter 12

Synthesis and characterization of inorganic materials to be used as adsorbents of toxic metals and of nuclear interest

English version of:

Capítulo 12

Síntesis y caracterización de materiales inorgánicos para ser empleados como adsorbentes de metales tóxicos y de interés nuclear

Published originally in the book:

Contribuciones del Instituto Nacional de Investigaciones Nucleares al Avance de la Ciencia y la Tecnología en México
Edición Conmemorativa 2010

Translation: Francisco Granados Correa

Synthesis and characterization of inorganic materials to be used as adsorbents of toxic metals and of nuclear interest

Francisco Granados Correa
Juan Serrano Gómez
Juan Bonifacio Martínez
Department of Chemistry, ININ
francisco.granados@inin.gob.mx

1. Introduction

This chapter reviews the development of the studies carried out in the ININ by Department of Chemistry investigators concerning water decontamination. The study of the metal separation in aqueous solution, through inorganic adsorbents, began in the Department of Chemistry with the use of zeolites to adsorb metal cations as Co and Cd. In1995, Nava et al. [1] studied the separation of Co and Cd, using zeolite X. Also studied was the adsorption capacity of the natural clinoptilolite to retain cobalt [2]. With the natural evolution of these works, the next step was to study the effect of organic compounds on the metal adsorption by zeolites, which was done by Solache-Rios et al., [3]. They investigated the effect of ethilendiamine on the cesium adsorption by zeolites 25M-5 and Y. Besides Co and Cd, the removal of Ni, Cd, and Zn from water with clinoptilolite and heulandite has also been investigated [4], as well as Hg separation with other zeolites [5]. In 2000 Serrano et al. [6] published an article on the ^{99}Mo adsorption in calcined hidrotalcita (CHT). Even though the purpose of the work was to develop a Tc-99m generator, we can say that with this study, the investigation to separate metallic anions using inorganic adsorbents started in the Department of Chemistry. In the recent years, Granados-Correa et al. [7, 8] have reported the separation of Cr in the form of chromate and dichromate ions (CrO_4^{2-}, $Cr_2O_7^{2-}$), using Fe-modified pozzolane and tricalcic phosphate. These studies found that both materials are highly efficient to separate chromium from aqueous solutions.

1.1. Contamination of water by heavy metals

Metals in their natural form are subjects to geochemical and biological processes that determine their presence and concentration in the components of the environment, such as grounds, underground, or superficial waters, atmosphere, and living beings. Diverse human activities have altered the concentration and natural presence of metals in the components of the environment, causing health problems to human beings, animals, and plants. Since water is indispensable to living beings, it is a fundamental task to keep it free of polluting agents so that it can be used without risks to health. Nevertheless, in the recent decades the water, mainly superficial water, has undergone an acute contamination caused by man's pouring of industrial, mining, and other wastes that contain diverse chemical substances into surface water bodies, with these wastes containing metals in varied chemical forms. Among the main metallic environmental polluting agents, we have As, Cd, Zn, Hg, Pb, Co, Cr and Ni, which have been classified as very toxic chemical elements that cause diverse damage to human health and to the ecosystem. Other metals also considered to be environmentally polluting are Be, Sb, Sn, Tl and Ti, even though their human toxicity is lesser [9-11].

1.2. Physicochemical methods for heavy metal removal in liquid effluents

The elimination of toxic chemical agents from water has become an essential subject with the accelerated development of industrial activities, in which the metallic salts form an important class

of polluting agents in the environment, on a large scale [12, 13]. For that reason, over the past few decades several methods have been used to decontaminate water and selectively to eliminate certain chemical species present in aqueous solution. The main techniques used to separate toxic agents from water are inverse osmosis, adsorption, ion exchange, chromatography, solvent extraction, and electrophoresis. In particular, the separation processes based on adsorption phenomena are important for eliminating trace elements, due to their high efficiency and selectivity.

1.2.1 Adsorption

Adsorption refers to the presence of any component on the surface of the solid phase in a higher concentration than that of any other component in the liquid phase (Figure 1). The substance deposited in the interphase is called adsorbate, and the substance in whose surface the adsorption happens, is called the adsorbent. In recent years a large number of new adsorbent materials have been investigated, including carbons, nanomaterials, new zeolites, aluminosilicates, clays, and porous solids [14-17]. All these materials have high specific areas (>100 m^2/g) and are highly porous, which is why they have been demonstrated effective for the treatment of radioactive and nonradioactive wastes in aqueous solution. These materials have an affinity to certain ions or ion groups and have shown high selectivity, resistance to degradation, high temperatures and high levels of radiation.

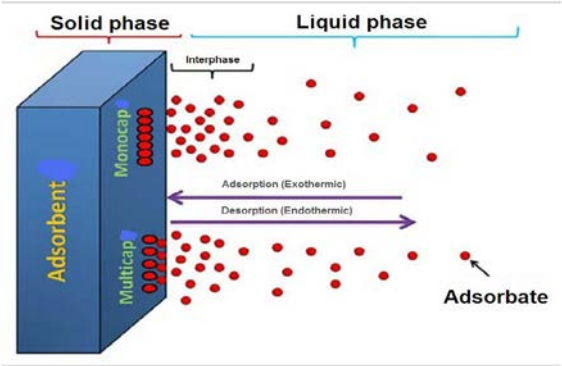

Figure 1. Adsorption process of an adsorbate on a solid surface.

1.2.1.1 Types of adsorption

In general, two main types of adsorption are well known: physical, or physicsorption, and chemical, or chemisorption.

Physicsorption means that the attractive forces are of a physical nature, and the adsorption is relatively weak. The forces correspond to those considered by J.H. van der Waals with respect to their equation of state for gases. The heat released when one mol of gas experiences physicsorption is generally low, less than 20 kJ [18].

Chemisorption was considered for the first time in 1916 by the chemist Irving Langmuir. Chemisorption means that the adsorbed molecules are bound to the surface by means of covalent forces, as in the atoms that form molecules. The heat released by the mol in this type of adsorption generally is comparable with that given off by a chemical bond, which is from 100 to 500 kJ/mol.

1.2.1.2 Physicochemical parameters that influence the adsorption processes

The efficiency of the adsorption processes depends on the characteristics of the adsorbent (specific area, structure, and size of particle, among others) and on the properties of the chemical species in solution (cations and anions, size of the ion, and electrical charge). The type of adsorption

mechanism that can happen between the phases, the conditions of the process (pH, temperature, concentration) and the forces that control the process (Van der Waals, electrostatic, chemical bonds) are also factors that influence the adsorption process.

2. Development and results

The toxic metal removal works carried out by investigators in the Chemistry Department at ININ are reviewed. In these works different absorbent solids such as pozzolane, calcium phosphate, and magnesium oxide, among others, have been used to study toxic metals adsorption, specifically chromium in its oxidation state VI and metals of nuclear interest.

Chromium presents several oxidation states, the most relevant, from a biological point of view, being oxidation states III and VI. The Cr(VI) presents greater toxicity for living beings than the Cr(III), even in low concentrations [9]. Contamination by chromium, specifically from Cr(VI), comes from wastes poured into superficial waters by tannery, dyes, pigments, and electrolytic chromium plating industries, among others. Once ingested, the hexavalent chromium is usually concentrated in the lungs. If ingested in high doses, it causes renal injuries. In agreement with the International Agency for Research in Cancer (IARC), Cr(VI) is classified as a powerful carcinogenic agent. Thus it is imperative to develop separation techniques to remove chromium from waste waters before the contaminated water is discharged outdoors, hence avoiding damage to the environment and consequently to humans.

2.1 CrO_4^{2-} ion adsorption on pozzolane modified with Fe

Pozzolane is a solid rich in silicates and aluminates, and when ferric ions are attached to the grain surface of these materials, their capacity to retain anions, such as the chromate ion present in watery wastes from tanneries, improves. In this study [8] the CrO_4^{2-} ion separation from 10^{-4} M K_2CrO_4 aqueous solutions was investigated by using Fe-modified pozzolane as adsorbent. The initial pH of the potassium chromate solution was 5.5. At a pH of 5.5, the Cr(VI) ions exist as the anions $HCrO_4^-$ and CrO_4^{2-} [19], which are adsorbed on the positively charged surface of the Fe-modified pozzolane, where groups-Fe-OH_2^+ are formed under the used acidic conditions. Hydroxyl groups adhere to the Fe when the modified solid material is contacted with aqueous solutions. Kinetic experiments have shown that the speed of adsorption is fast at the beginning of the separation process, and that the equilibrium in the distribution of the ion chromate was reached in approximately 2 h (figure 2). In these equilibrium conditions, the CrO_4^{2-} ion adsorption on the Fe-modified pozzolane was 3.23×10^{-3} mmol/g.

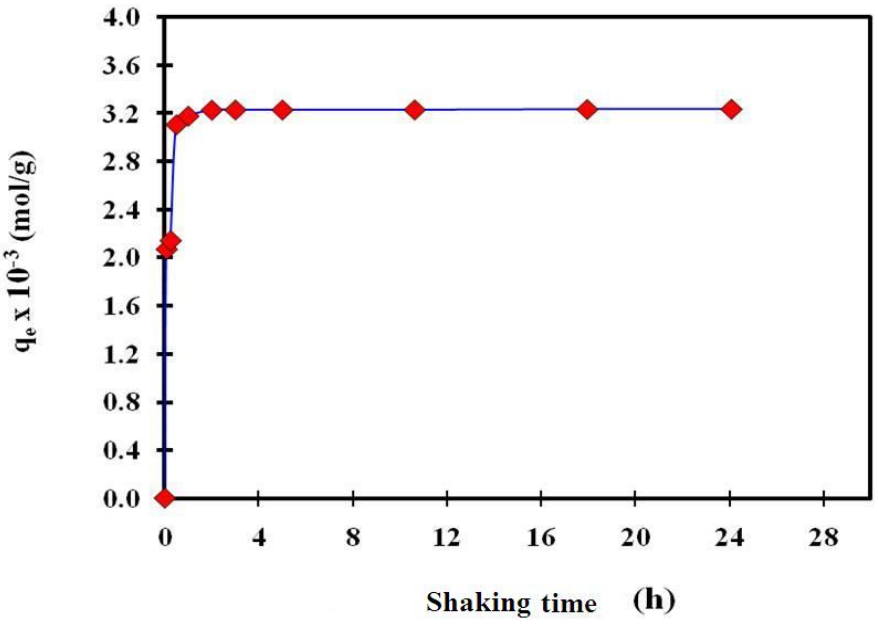

Figure 2. Shaking time effect on CrO_4^{2-} ion adsorption on Fe-modified pozzolane

The adsorption data as a function of Cr(VI) ion concentration were analyzed with the isotherm models of Freundlich, Langmuir, and Dubinin-Radushkevich (D-R), and it was found that they fit the three types of isotherm models.

The Freundlich model equation in its linear form is:

$$log\ a_e = 1/n\ log\ C_e + log\ K_{F,} \qquad (1)$$

where a_e and C_e are the amount of CrO_4^{2-} ions adsorbed (mol/g) and the bulk concentration (mol/L) at equilibrium, respectively, and $1/n$ and K_F are the constants of Freundlich that refer to adsorption capacity and adsorption, respectively. Figure 3 is a plot of log a_e versus log C_e. The obtained straight line indicates the validity of the isotherm of Freundlich for the obtained adsorption data. From the slope and intercept of the line, the numerical values of the Freundlich constants, i. e., $1/n$ and K_F were determined, and the obtained values were: $1/n$ =0.67 and K_F =3.58x10^{-3} mol/g. The value of $1/n$, less than unity, indicates a heterogeneous surface structure of the adsorbent and a non-appreciable interaction between the adsorbed species. In general, as the K_F values increases, the adsorption capacity for the given adsorbent, also increases.

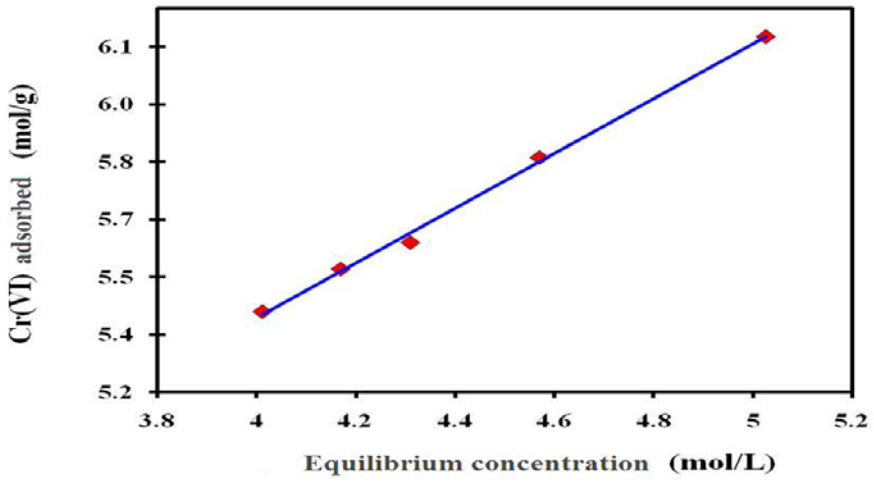

Figure 3. Freundlich isotherm of CrO_4^{2-} ion adsorption on Fe-modified pozzolane

Langmuir's equation in its linear form is as follows:

$$C_e/a_e = 1/ka_{max} + C_e/a_{max,} \quad (2)$$

where C_e and a_e have the same meaning as in the equation of Freundlich, and k and a_{max} are the Langmuir constant related to the energy of adsorption and to the maximum adsorption capacity, respectively. A straight line was obtained when C_e/a_e was plotted versus C_e. The slope of this straight line gives the value of a_{max} = 5.78x10^{-6} mol/g, and the intercept yields the value of k =1.58 x10^6 L/mol.

In order to understand the nature of the adsorption process, the model of the Dubinin- Radushkevich isotherm (D-R) in its linear form was also verified:

$$ln\ a_e = ln\ a_{max} - Ke^2. \quad (3)$$

Here a_{max} is the maximum amount of CrO_4^{2-} ions that can be adsorbed on Fe-modified pozzolane under the optimal experimental conditions, K is a constant related to the ion adsorption energy (mol^{-1} kJ^{-2}), and e is the potential of Polanyi (kJ/mol), which is calculated using the following equation:

$$e = RT\ ln(1 + 1/C_e), \quad (4)$$

where R is the gas constant, 8.314 J/mol K, T is the absolute temperature in Kelvin degrees, and C_e is the concentration at equilibrium of the residual chromate ions. The plot of $ln\ a_e$ against e^2 gave a straight line. The mean free energy of adsorption E, defined as the free energy of the transfer of one mol of solute from the infinite (in solution) to the surface of Fe-modified pozzolane grains, was calculated with the relation $E=1/\sqrt{(-2K)}$, being the found value of E =9.44±0.07 kJ/mol with K =-5.60x10^{-3} mol^2/kJ^2. The E value indicates that the adsorption presents a low potential energy barrier. This value is more consistent with a physical adsorption process.

The effect of temperature on the adsorption of CrO_4^{2-} ions was investigated by varying the temperature from 293 to 323 K. Using the obtained adsorption data, changes in standard enthalpy (ΔH^0), standard entropy (ΔS^0), and Gibbs free energy (ΔG^0) were evaluated, using the following equations:

$$log\ K_d = (-\Delta H^0/2.303R)(1/T) + \Delta S^0/2.303R \quad (5)$$

$$\Delta G^0 = -\ RT\ ln\ K_d \quad (6)$$

$$\Delta G^0 = -\ \Delta H^0 - T\Delta S^0, \quad (7)$$

where K_d is the distribution coefficient [20], T the temperature in Kelvin (K), and R the gas constant. Fig. 4 shows a plot of log K_d vs 1/T. The straight line of that figure can be described by the van´t Hoff equation in its linear form:

$$log\ K_d = (-\Delta H^0/2.303R)(1/T) + constant \quad (8)$$

The slope ($-\Delta H^0/2.303R$) of the straight line in Fig. 4 was computed by using the least square technique. By a simple calculation with R = 8.31434 kJ/K·mol and the numerical value of the slope, the change in the enthalpy (ΔH^0) of the chromate ion adsorption was found to be 49.87 kJ/mol; and the positive value opposes the chromium adsorption, which is due to a large enthalpy required for dehydration of the metal ion to be adsorbed on the Fe-modified pozzolane, additionally indicating the endothermic nature of adsorption [21]. On the other hand, the value of change in the entropy (ΔS^0) of the system was estimated to be 19.81×10^{-2} kJ/K·mol, and the positive value indicates that the degree of freedom of ions is increased by adsorption. The value of change in Gibbs free energy (ΔG^0) was found to be -8.17± 0.3 kJ/mol; the negative change in energy reveals that the uptake process is spontaneous.

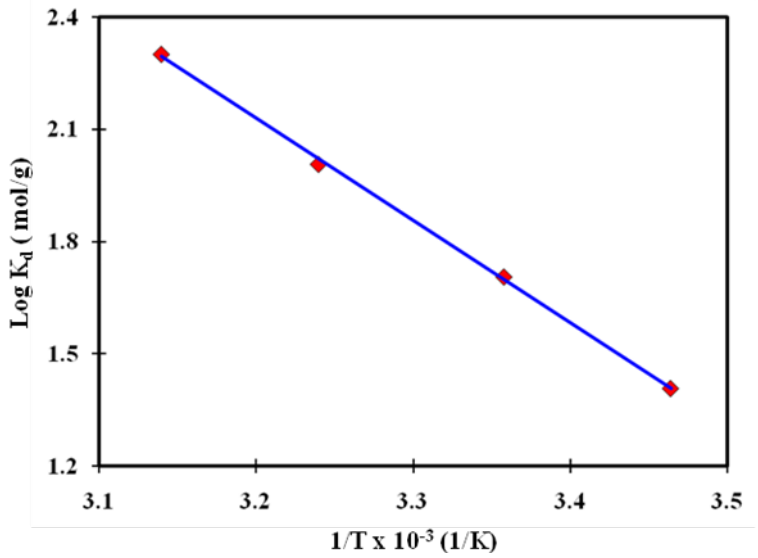

Figure 4. log K_d vs *1/T* for CrO_4^{2-} ion adsorption on Fe-modified pozzolane

This study showed the ability of the Fe-modified pozzolanne to adsorb CrO_4^{2-} ions from an aqueous solution. The adsorption was found to be dependent on the initial concentration and temperature in the equilibrium. Experimental isotherms of CrO_4^{2-} ions were adequately modeled by Freundlich,

Langmuir, and Dubinin-Radushkevich (D-R) isotherms over the entire concentration range studied. The positive value of ΔH^0 indicates the endothermic nature of adsorption; the positive value of ΔS^0 indicates the increasing randomness of the system; and ΔG^0 proves that the adsorption of CrO_4^{2-} ions on Fe-modified pozzolane is a spontaneous process. The Fe-modified pozzolane can be effectively used for the removal of CrO_4^{2-} ions from aqueous solution and in the treatment processes of industrial wastes.

2.2 Adsorption of Cr(VI) ions on tri-calcium phosphate

In the search for new materials to be used in the removal of CrO_4^{2-} ions from aqueous solutions, tri-calcium phosphate has been investigated. The synthesized material was surface and structure characterized. The results obtained are described in the following paragraphs.

Tri-calcium phosphate was synthesized using the continuous precipitation method reported by Gómez-Morales et al. [22]. Monobasic ammonium phosphate and calcium nitrate were utilized. The obtained material was dried at 120 ºC for 2.5 h and heated at 1050 ºC for 2.5 h. The X-ray diffraction analysis showed that the synthesized material has the crystalline structure of hydroxyapatite [$(Ca_{10}(PO_4)_6(OH)_2)$]. No other crystalline phase was observed. The parameters of the crystalline net were calculated with the aid of the method described by Survnarayama et al. [23], and they were found to be a = b = 9.385 Å and c = 6.870 Å. According to the calculations carried out with the Sherrer equation, tri-calcium phosphate has an average grain size of 75 nm. The infrared spectroscopy analysis showed the presence of the PO_4^{3-} group, structural OH^- groups, and probably a very small amount of calcium carbonate [24]. In general, the obtained IR spectrum depicts the high purity of the analyzed calcium phosphate.

The thermal gravimetric analysis initially showed the usual moisture loss at 43 ºC and crystallization water at 150 ºC. Another mass loss was observed at 360 ºC, which may be due to the decomposition of carbonate ions. These carbonate ions are previously formed in the calcium phosphate from the absorbed CO_2 in the material. Finally, two more mass losses are detected at 642 and 697 ºC, as a result of the decomposition of the phosphate groups

The hydroxyapatite micrographs obtained with the scanning electronic microscope exhibit a material with a particle size interval from 5 to 40 μm, which indicates a size high dispersion. The semiquantitative analysis, carried out with the EDS technique, indicated that the elemental composition for the synthesized material was P = 27.47%, Ca = 19.64%, and O = 52.89%.

The removal of CrO_4^{2-} ions from aqueous solution, using the tri-calcium phosphate, was studied through batch experiments as a function of contact time, initial pH of the chromate solution, amount of adsorbent, chromium concentration, and temperature. Fig. 5 displays the adsorption of Cr(VI) ions on calcium phosphate. It can be observed that the equilibrium in the adsorption process is reached in 24 h of contact time between the solid and aqueous phases.

The adsorption of Cr(VI) ions at equilibrium was favored at high temperature and acidic pH values. To study the effect of chromium concentration on Cr(VI) adsorption, a concentration interval from $5x10^{-4}$ to $5x10^{-5}$ M was used. The experimental adsorption data of Cr(VI) fit the Freundlich, Langmuir, and Dubinin-Radushkevich (D-R) isotherms models. The values of Freundlich constants *K* and *1/n* were calculated as described above, and the obtained values were $4.6x10^{-2}$ mol/g and 0.67, respectively. The value of *1/n* (less than unity) found in this work confirms that the isotherm of Freundlich is valid for the Cr(VI) ion adsorption data, which suggests that the adsorbent surface is heterogeneous with an exponential distribution of the active sites. Regarding the Langmuir isotherm, the slope (maximum retention capacity) of the straight line was $a_{max} = 2.0 \pm 0.01x10^{-4}$

mol/g, and the interception was K = 5.42 ± 0.1x10^2 dm^3/mol, with a correlation coefficient R^2 = 0.9995. In relation to the D-R isotherm, the obtained values of the maximum amount of chromium that can be adsorbed on calcium phosphate, as well as the mean energy of adsorption, obtained from the slope and interception of the corresponding straight line, were found to be a_{max} = 8.5 ± 0.04x10^{-4} mol/g and E = 7.7 ± 0.10 kJ/mol, respectively.

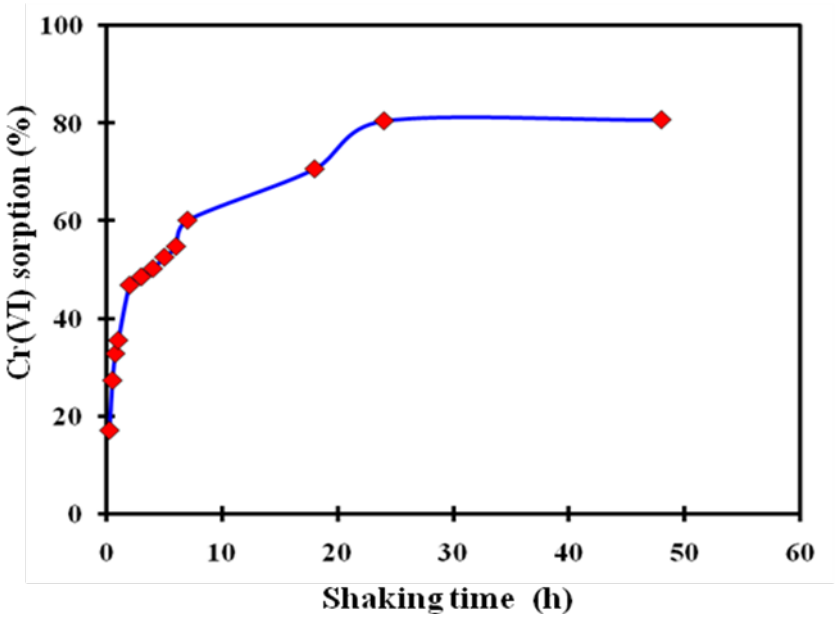

Figure 5. Sorption of Cr(VI) ions on calcium phosphate as a function of shaking time

The pH effect on the adsorption of Cr(VI) ions onto calcium phosphate was investigated by batch experiments. Chromium solutions with pH from 3 to 11 were used. The pH values were adjusted with concentrated HNO_3 and NaOH aqueous solution. The obtained results are shown in Fig. 6. The chemical species of chromium are anionic species, and their adsorption decreased when the pH was increased to alkaline values. The maximum chromium adsorption was observed at slightly acidic pH values (from 4 to 5). In acidic media, the chromium chemical species present in solution are $HCr_2O_7^-$ or $Cr_2O_7^{2-}$ [25], which are adsorbed on the electrically charged positive surfaces of calcium phosphate, leading to high percentages of chromium adsorption. The Cr(VI) ions in solution interact with the groups OH_2^+ and OH, which are present on the solid surface when the aqueous media are acidic and alkaline, respectively. The adsorption data of chromium at equilibrium and as a function of temperature were used to calculate the thermodynamic parameters ΔH^0, ΔS^0, and ΔG^0 of the adsorption process, by means of the corresponding equations also described above. The values of these parameters are as follows: ΔH^0 = 14.3 ± 0.3 kJ/mol, whose positive value shows the endothermic nature of the adsorption process. The magnitude of ΔH^0 is related to the reaction mechanism. If ΔH^0 is in the interval 8-16 kJ/mol, the adsorption is controlled by an ionic exchange. ΔS^0 = 12.8 ± 0.2x10^{-2} kJ/Kmol, and its positive value, indicates an increase in the randomness around the interface liquid/solid by the fixation of chromium ions on the calcium phosphate. When the ions are adsorbed on the calcium phosphate surface, the water molecules which were previously bound to the metallic ions are released and dispersed in the solution, resulting in an increase in the entropy. The negative sign of ΔG^0 = -23 ± 2.0 kJ/mol indicates the spontaneity of the adsorption process.

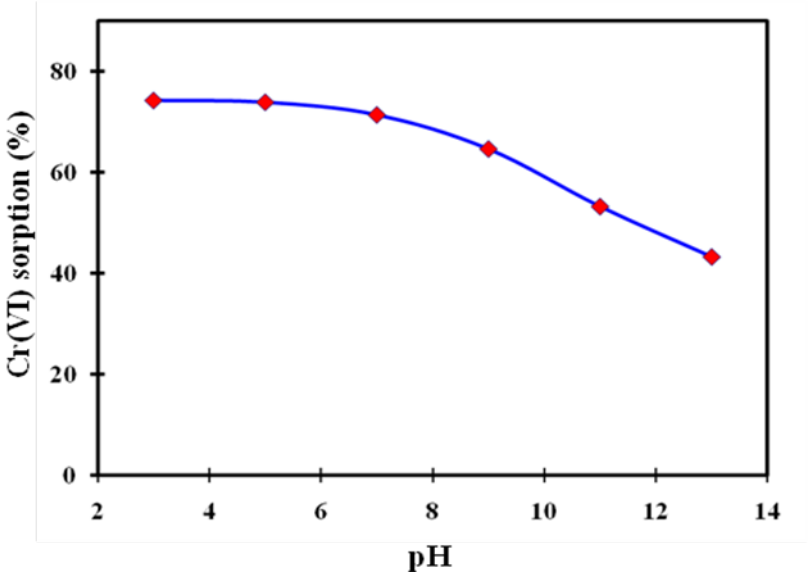

Figure 6. Adsorption Cr(VI) ions on calcium phosphate as a function of pH

In summary, for this study calcium phosphate was prepared and characterized. The equilibrium in adsorption was reached in about 24 h. The chromium adsorption process is controlled by an ion exchange reaction. The Cr(VI) ion adsorption at equilibrium was favored at high temperatures and slightly acidic pH values. The experimental Cr(VI) adsorption isotherms fit the Freundlich, Langmuir, and D-R isotherms models. The adsorption mean energy was calculated by using the D-R adsorption isotherm in its linear form. The signs of ΔH^0, ΔS^0 and ΔG^0 indicate the endothermic and spontaneous nature of the chromium adsorption process. These results show that calcium phosphate is an efficient adsorbent to remove Cr(VI) ions from aqueous solutions.

2.3 Ball milling effect of calcium phosphate on its chromium adsorption properties

The specific surface of a solid material is related to the number of surface active sites available for retaining chemical species to be separated from contaminated aqueous solutions. Thus, calcium phosphate synthesized in the laboratory presents a high ability to adsorb Cr(VI) species due to its high specific surface: 64.5 m^2/g. As mentioned before, with the help of the corresponding XRD pattern and the Sherrer equation a grain size of 75 nm was obtained for the synthesized calcium phosphate. This grain size cannot be considered as small, and reducing it by fragmentation to smaller values can improve the calcium phosphate adsorption properties because the obtained material could have a higher specific surface. A high energy mill can be used for carrying out the material fragmentation [26]. With the fragmentation process, the morphology and particle size of solid material samples can be modified by varying the milling time; then the new values of these parameters can be compared with those of non-milled calcium phosphate samples, all samples having been previously prepared by the continuous precipitation method. To determine the effect of changes on the surface structure of calcium phosphate on its adsorption properties, the Cr(VI) ion adsorption on pulverized calcium phosphate was investigated as a function of fragmentation and liquid-solid contact time.

The synthesized and dried material was milled with a ball mill of high energy (Spex, model 8000). The samples of calcium phosphate (TCP) were milled for various times 5, 10, and 15 h, and the milled samples were named TCP-5, TCP-10, and TCP-15. The non-milled sample was called only TCP. The milling was carried out under normal atmosphere with 9 stainless steel balls (1/4 in

diameter) mixed with 18 stainless steel balls (3/16 in diameter). The ball to powder weight ratio was 6:1, and methanol was used as the lubricant agent (0.25 mL). Once the mechanical milling was ended, the samples were characterized, and then the removal of Cr(VI) ions from aqueous solutions by the fragmented solids was studied. The solids were characterized by XRD, SEM, EDS, and specific surface measurements.

The XRD patterns of non-milled and fragmented TCP samples correspond to the structure of hydroxyapatite (file 9-0432, JCPDS). The XRD patterns of milled samples showed broader and slightly less intense peaks, as compared to non-fragmented TCP samples, as the milling time was increased from 0 to 15 h. The broader peaks in the fragmented samples indicate a decrease in the crystallite size, decreasing from 57 nm in the non-milled TCP sample to 13 nm in the sample TCP-15. Again, the particle size was calculated with the help of the Sherrer equation.

The SEM results showed that the size and shape of the grains in samples TCP, TCP-5, TCP-10, and TCP-15 are different from each other. The grains in the original sample (TCP) are long with a smooth surface and a grain size around 10 μm. The grain size of the TCP-5 sample is less than 10 μm, they are homogeneous and form conglomerates. Samples TCP-10 and TCP-15 also form conglomerates, and some of them are bigger than in sample TCP-5.

The specific surface areas measurements revealed that the TCP sample has a specific surface of 60.5 m^2/g, while the corresponding values for the; milled samples are TCP-5, 19 m^2/g, TCP-10, 14 m^2/g; and TCP-15, 12 m^2/g. These data indicate that the specific surface of calcium phosphate decreased with the milling time. In the same way, the total pore volume in the calcium phosphate decreased from 0.2053 to 0.0256 cm^3/g, as the milling time varied from 0 to 15 h.

Regarding the Cr(VI) ion adsorption on calcium phosphate, the retention at equilibrium of Cr(VI) ions is as follows: TCP, $8.1x10^{-4}$ meq/g; TCP-5, $11.4x10^{-4}$ meq/g; TCP-10, $12.0x10^{-4}$ meq/g; and TCP-15, $14.0x10^{-4}$ meq/g. As can be seen, an increase in milling time resulted in an increase of chromium retention.

The particle size in the milled samples decreased with the milling time due to the fracture in the particles, which was caused by the high energy impact of the steel balls during the milling. An increase of the specific surface in the fragmented samples was expected with an increase in the milling time because of the decrease in the particle size; however, the obtained results displayed an opposite behavior. An explanation of these unusual results is as follows: In addition to the described fracture, the fragmented particles must have undergone a compression from the steel balls, so that the pores of these particles were reduced in volume, thus causing a reduction of the total pore volume, and consequently a reduction of the specific surface area values in the milled TCP samples. The observed reduction of the total pore volume with milling time confirms the explanation given for the unexpectedly low values of the specific surface areas of the milled samples.

On the other hand, it is well known that the higher the specific surface area of an inorganic adsorbent, the higher the retention of cations or anions on the adsorbent [7]. As described above, this study found a reduction in the specific surface area with an increase in milling time, and for this reason a decrease of ion adsorption on the fragmented TCP samples was expected; however, the opposite was observed: Cr(VI) ions were increasingly adsorbed in the milled samples as the specific surface area values decreased. This apparent contradiction can be explained by the presence of Fe in the calcium phosphate milled samples, as this chemical element was found in the XRD patterns and the EDS results. The presence of Fe in the TCP fragmented samples must come from the steel balls of the high energy mill. It should be noted that Fe is present in the TCP-15 fragmented sample in

considerable amounts. The peak, centered at 45º in 2θ degrees of the X-ray pattern, is intense and corresponds to Fe. In our study, such a condition can facilitate the Cr(VI) ion sorption, since the Fe present in the milled TCP samples modifies their particle surface. In sorption processes, the sorption of metal ions on mineral surfaces may occur because of metal ion interaction with attached functional groups, such as hydroxyl groups, on the mineral surfaces. These hydroxyl groups are formed when the adsorbent material is contacted with aqueous solutions. The adsorption behavior of the fragmented calcium phosphate has been previously observed in Fe-modified zeolites when this modified material was used to remove arsenate ions [9] from aqueous solutions; i. e., the arsenate adsorption was enhanced by the presence of Fe on the zeolite surface.

In summary, the ball milling results in TCP samples of very small particle size (less than 20 nm). As milling time increased to 15 h, the particle size and the specific surface area of the milled TCP samples decreased because the small particles were compacted by the strokes of the highly energized steel balls of the mill. This compression caused the pores of the TCP particles to be reduced in volume, effecting a reduction of the total pore volume and, consequently, a reduction in the specific surface area of the ball-milled TCP samples. On the other hand, the chromium (VI) sorption on milled TCP samples unexpectedly increased, as the specific surface area became smaller. The presence of Fe originating from the steel balls in the milled samples explains the increase of Cr(VI) sorption. Fe is deposited on TCP nanometric particles, causing an enhanced Cr(VI) sorption through the interactions of these ions with the hydroxyl groups attached to Fe atoms [26].

2.4 Cobalt sorption on MgO prepared by solution combustion

The MgO synthesis was carried out by using the solution combustion method [7]. Some parameters of the synthesis method were varied, and later the morphology of the obtained MgO was compared with that of an MgO sample prepared by calcinations of magnesium nitrate. To test the surface structure variations, the cobalt sorption, often found in wastewaters from nuclear industries, was studied by means of batch experiments.

The MgO was obtained by the solution method, starting from mixtures of 0.2 g of $Mg(NO_3)_2{\cdot}6H_2O$ and 0.4 g of urea. The mixtures were suspended in 0.5, 1.0, 1.5, 2.0 2.5, and 3.0 mL of water to obtain a homogeneous solution. Then, the mixtures were heated to evaporation and later calcined in a muffle furnace at 800 ºC for 5 minutes. Another sample of MgO was prepared by the calcination method, where 0.5 g of magnesium nitrate inside a 30 mL crucible was heated for 2 h in the muffle furnace, also at 800 ºC. Table 1 shows the compounds identified by XRD in the MgO samples obtained by both methods. The corresponding specific surface areas are also shown.

Table 1. Chemical compounds identified by XRD in MgO synthesized samples. BET specific surface areas are also shown.

Sample	Synthesis	Treatment	Compounds	Surface area (m^2/g)
0	Calcined MgO	Calcination	MgO (periclase)	1.7
A	Combustion synthesis	Combustion	MgO (periclase) + non-crystalline	28.0
B	MgO-H_2O (1 mL)	Solution combustion	MgO (periclase) + non-crystalline	52.0
C	MgO-H_2O (2 mL)	Solution combustion	MgO (periclase) + non-crystalline	51.0
D	MgO-H_2O (3 mL)	Solution combustion	MgO (periclase) + non-crystalline	45.0

The MgO fractal dimension was obtained by Small Angle X-Ray Scattering (SAXS). The fractal dimension, which describes the amount of roughness and porosity on material surfaces, can have any value between 2 <d< 3. Dimension fractal values below 2 indicate smooth surfaces; slightly higher values indicate irregular surfaces; and values close to 3 indicate very irregular or rough surfaces.

Table 2 shows the results obtained by SAXS, MEB and BET, where it can be seen that MgO samples prepared by combustion (sample A) and solution combustion methods (samples B, C, and D) are the more fractally structured oxides (2.3), and instead sample 0 has a fractal dimension of 3.0. These values, which are volume fractal dimensions, show that the connectivity of the magnesia structure depends on the preparation method.

Table 2. Comparation of the results by SAXS, SEM and BET

Sample	Radial distribution function (XRD)	Shape of heterogeneities (SAXS)	Fractal dimension (SAXS)	Pore size distribution, maxima in Å (SAXS)	Particle morphology (SAXS)	Surface fractal dimension (BET) R^2
0	MgO structure only	Spheres	3.0	45, 70, 100	No defined morphology	2.0 (R^2 = 0.9616)
A combustion Synthesis	MgO structure only	Lamellae	2.3	Broad, 70	Homogeneous, small particles (ca. 0.1 μm)	1.8 (R^2 = 0.9967)
B (1 mL)	MgO structure only	Lamellae	2.3	Broad, 70	Large bubbles, lamellar	1.7 (R^2 = 0.9968)
C (2 mL)	MgO structure only	Lamellae	2.3	Broad, 70	Bubbles, slightly more compact, lamellar	1.7 (R^2 = 0.9988)
D (3 mL)	MgO structure only	Lamellae	2.3-2.5	Broad, 70	Much more compact, some particles ca. 0.1 μm	1.7 (R^2 = 0.9973)

The shape and size of the grains of synthesized MgO samples determined by SEM are very different (Fig. 7). The particles of the calcined sample are so large that no texture is observed. The surface is smooth and is typical of a well-crystallized material. The combustion prepared MgO presents homogeneous particles whose size is close to 0.1 μm.

The specific surface area of calcined MgO turned out to be 1.7 m^2/g, whereas all other samples presented areas comprising between 28 and 52 m^2/g. The highest value was 52 m^2/g, obtained for the MgO prepared by combustion with 1 mL of water. A variation of 1 mL of water (from 2 to 3 mL) diminishes the surface area in more than 25%; therefore, the control of combustion reaction through water is essential for obtaining high specific surface areas. Fig. 8 correlates the specific surface area of MgO samples obtained by combustion with the amount of water added during the synthesis.

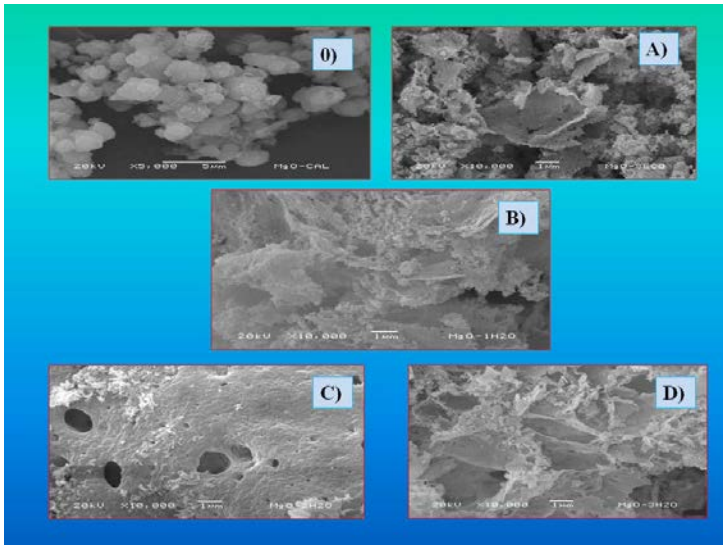

Figure 7. SEM images of the MgO samples: 0) calcined MgO,
A) combustion MgO, B) MgO-H_2O, C) MgO-$2H_2O$, D) MgO-$3H_2O$

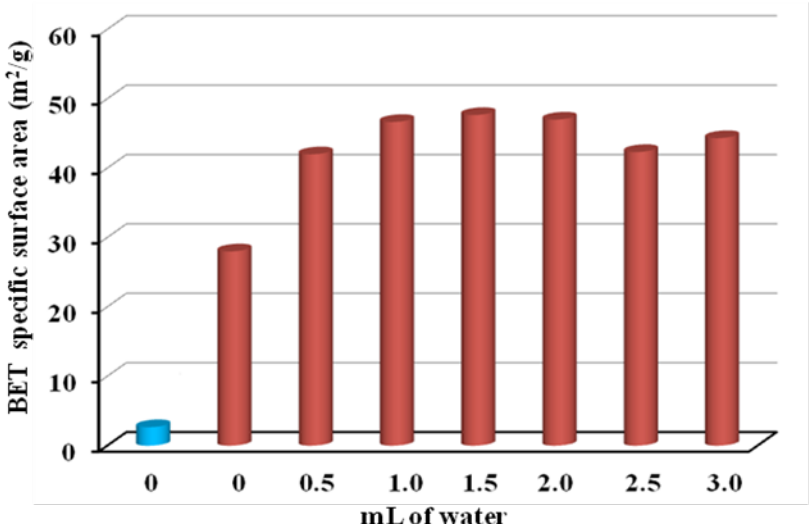

Figure 8. BET specific surface areas of MgO samples prepared by combustion and solution combustion, as a function of water amount added during the synthesis

When the surface fractal dimension was obtained from the N_2 adsorption data, the value for calcined MgO (sample 0) was 2.0 and for the combustion prepared samples was 1.8. For the solution combustion samples, B, C, and D, the value was 1.7, as shown in Table 2 and Fig. 9. The above results indicate that the pores on the material surfaces are regulars, bearing more active sites that facilitate an adsorption process.

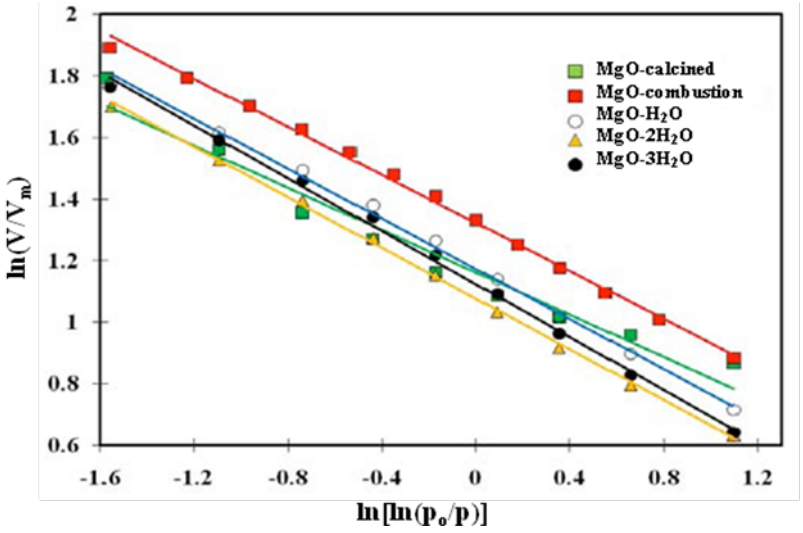

Figure 9. $\ln(V/V_m)$ vs $\ln[\ln(p^o/p)]$ to determine the fractal surface: calcined MgO, combustion MgO, MgO-H_2O, MgO-$2H_2O$ and MgO-$3H_2O$

Batch experiments were carried out at room temperature mixing, in closed vials, 0.1 g of each MgO and 10 mL of $^{60}Co^{2+}$ solution at pH of 5.5. Samples were stirred for 10 s and shaken for 1 h. The liquids were separated from the solids by centrifugation (5 min at 3000 rpm). The radioactivity of $^{60}Co^{2+}$ in each aliquot of 5 mL was measured with an Ortec Ge/hyperpure solid state detector coupled to a multichannel analyzer. Radioactive $^{60}Co^{2+}$ was obtained by thermal neutron irradiation of a $Co(NO_3)_2 \cdot 6H_2O$ for 1 h in the Triga Mark III nuclear reactor at the Mexican Nuclear Center, with a neutron flux of 10^{12}-10^{13} n/cm^2 s. Fig. 10 shows the cobalt retention on each prepared sample, and the values were found to be as follows: calcined MgO (sample 0), 2.1%; combustion MgO (sample A), 25.0%; sample B, 32.5%; sample C, 32%; and sample D, 29%.

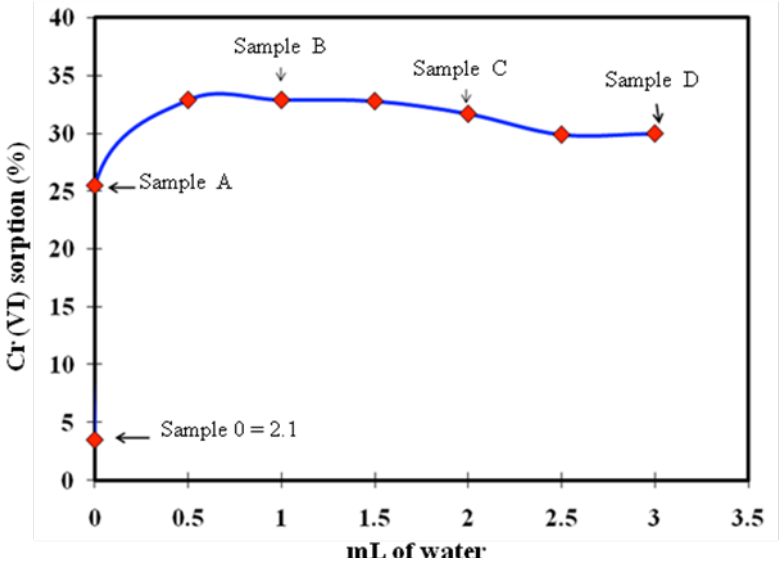

Figure 10. Co^{2+} sorption capacity of MgO obtained by combustion and combustion in solution. Co concentration: $1x10^{-4}$ M, room temperature

To summarize, in this study MgO was prepared by combustion with urea. This material presented a specific surface area of 28 m^2/g, a value much higher than that of the MgO obtained by calcinations, 1.7 m^2/g. The use of water in the MgO synthesis produces materials with higher specific surface areas, from 45 to 52 m^2/g, and Co^{2+} retention capacity. The sample prepared by combustion with 1 mL of water presented the highest Co^{2+} retention (32 %). The sample morphology depended on the amount of added water, and laminar structures with large craters were observed. The samples obtained with 2 mL of water were shown to be denser than those obtained with 1 mL of water. The sample prepared with 3 mL of water was much more compact, although small particles (about 0.1 nm in size) were observed. The material prepared with 1 mL of water (specific surface area: 52 m^2/g, surface dimension of fractal: 1.7, with laminar morphology and wide dimensional distribution of particle centered at 70 Å) presented the best Co^{2+} retention. Possibly, with more added water, a fraction of combustion heat might be used to evaporate the water excess, as deduced from the craters observed in the images obtained by SEM.

3. Research work in prospect

Continuing with the research work of separating toxic metals from aqueous solutions by their adsorption on inorganic solids, adsorption properties of other materials such as Bohemite [27], MnO_2 [28], ZnO [29], and $BaCO_3$ [30] have been investigated. In the future, we will investigate the removal of arsenic and chromium anions from aqueous solutions by their adsorption on iron phosphate. Hydroxyl groups attach on surface iron atoms of iron phosphate when this material is suspended in water, and the hydroxyl groups work as active sites to retain anions by electrostatic attraction in acidic media or are substituted as OH^- ions by toxic anions in alkaline media. Thus, higher chromate ion retention is expected with iron phosphate, as well as high arsenate retention.

Finally, as MgO is highly efficient to separate toxic metals in aqueous solutions, as found for Co^{2+}, we will continue investigating the use of this adsorbent material to separate polluting metal cations, such as the Cd^{2+}, Zn^{2+}, Hg^{2+}, Ni^{2+} and Pb^{2+} present in aqueous solutions.

References

1. Nava I, García-Sosa I, Solache-Ríos M. Removal of Co and Cd by zeolita X. J. Radioanal. Nucl. Chem. **191**, 83-87, 1995.
2. Hernández-Barrales E, Granados-Correa F. Sorption on radioactive cobalt in natural mexican clinoptilolite. J. Radioanal. Nucl. Chem. **242**, 111-114, 1999.
3. Solache-Ríos M, García-Sosa I, Sosa-Reyes S. Ethylen diamine effect on the sorption of cesium on zeolites 25M-5 and Y. J. Radioanal. Nucl. Chem. **237**, 83-87, 1998.
4. Pavón TB, Campos E, Sánchez Millán G, Olguín MT. Remoción de Ni, Cd y Zn del agua, utilizando clinoptilolita-heulandita. Ergo Sum **7**, 259-265, 2000.
5. Moreno GY, Olguín GMT. Separación de Hg (en presencia de Ag, Zn y Cu) en agua por la clinoptilolita-heulandita del estado de Gro. Informe Técnico. ININ, CB005/01 (2000).
6. Serrano GJ, Vertín MV, Bulbulian S. ^{99}Mo sorption by thermally treated hydrotalcites. Langmuir **16**, 3355- 3360, 2000.
7. Granados-Correa F, Bonifacio-Martínez J, Lara VH, Bosch P, Bulbulian S. Cobalt sorption properties of MgO prepared by solution combustion. Appl. Surf. Sci. **254**, 4688- 4694, 2008.
8. Granados-Correa F, Serrano-Gómez J. CrO_4^{2-} ions adsorption by Fe-modified pozzolane. Sep. Sci. Technol. **44**, 924-936, 2009.

9. Payne BK, Abdel-Fattah MT. Adsorption of arsenate and arsenite by iron-treated activated carbon and zeolites: Effects of pH, temperature, and ionic strength. J. Environ. Sci. Heal. A. **40**, 723-749, 2005.
10. IARC (Internacional Agency for Research on Cancer). Monographs on the evaluation of the carcinogenic risk of chemicals to humans. Lyon, France, 1993.
11. Verma A, Chakraborty S, Basu JK. Adsorption study of hexavalent chromium using tamarind-hull based adsorbent. Sep. Purif. Technol. 50, 336-341, 2006.
12. El-Hammari L, Laghzizil A, Saoiabi A, Barboux P, Meyer M, Brandes S, Guilard R. Some factors affecting the removal of lead (II) ions from aqueous solution by porous calcium hydroxyapatite: Relationships between surface and adsorption properties. Adsorp. Sci. Technol. **24**, 507-516, 2006.
13. Singh N, Singh PN, Hershman JM. Effect of calcium carbonate on the absorption of levothyroxine J. Am. Med. Assoc. **238**, 2822-2825, 2000.
14. Ambe, S. Adsorption of No-carrier-added $^{119}Sb(V)$ ions onto metal oxide and hydroxide surfaces from aqueous solutions. Radiochim. Acta. **46**, 145-150, 1989.
15. Kim DW, Kim CS, Lee NS, Ryu HI. Chromatographic separation of lithium and magnesium isotopes by manganese (IV) oxide. Radiochim. Acta. **90**, 179-183, 2002.
16. Tochiyama O, Yamazaki H, Mikami T. Sorption of neptunium(V) on various aluminum oxides and hydrous aluminum oxides. Radiochim. Acta. **73**, 191-198, 1996.
17. Abe M. Oxides and hydrous oxides of multivalent metals as inorganic ion exchange materials. Boca Raton, Fl, EUA: CRC Press, 1982.
18. Laidler K, Meiser J. Fisicoquímica, Nueva York, EUA: Continental, 2003.
19. Puigdomenech I. Program MEDUSA: Make equilibrium diagrams using Sophisticated Algorithms. http:/www.inorg.Kth.se/Research/Ignasi/Oindex.html, 1999.
20. Serrano GJ, García DOC. Ce^{3+} adsorption on hydrated MnO_2. J. Radioanal. Nucl. Chem. **230**, 33-37, 1998.
21. Kilislioglu A, Bilgin B. Adsorption of uranium on halloysite. Radiochim. Acta. **90**, 155-160, 2002.
22. Gómez-Morales J, Torrent-Burgués J, Boix T, Fraile J, Rodríguez-Clemente R. Precipitation of stoichiometric hydroxyapatite by a continuous method. Cryst. Res. Technol. **36**, 15-26, 2001.
23. Suryanarayana C, Norton MG. X-ray diffraction. A practical approach. New York, USA: Plenum Press, 1998.
24. Nakamoto K. Infrared Spectra of Inorganic and Coordination Compounds. New York, USA: John Wiley & Sons, Inc., 1963.
25. Baes FC, Mesmer RE. The hydrolysis of cations. New York, USA: John Wiley and Sons Inc, 1976.
26. Granados-Correa F, Bonifacio-Martínez J, Serrano-Gómez J. The ball milling effect on tribasic calcium phosphate and its chromium (VI) ion. J. Chilean Chem. Soc. **52**,252-255, 2009.
27. Granados-Correa F, Jiménez-Becerril J. Chromium (VI) adsorption on boehmite. J. Hazard. Mater. **162**, 1178-1184, 2009.
28. Granados-Correa F, Jiménez-Becerril J. Adsorption of $^{60}Co^{2+}$ on hydrous manganese oxide powder from aqueous solution. Radiochim. Acta. **92**, 105-110, 2004.
29. Alvarado-Ibarra Y, Granados-Correa F, Lara VH, Bosch P, Bulbulian S. Nickel (II) sorption on porous ZnO prepared by solution combustion method. Colloid Surfaces A: Physicochem. Eng. Aspect. **345**, 135-140, 2009.
30. Rosas-Gutiérrez N, Granados-Correa F, Bulbulian S. ^{60}Co adsorption on $BaCO_3$. Int. Nucl. Chem. Soc. News. **5**, 35-41, 2009.